Structural Eng. / Earthquake Eng. Vol. 6. No. 1, 69s- 77s. April 1989
Japan Society of Civil Engineers (Proc. of JSCE No. 404/I-11)

BUCKLING OF AN ANNULAR SECTOR PLATE SUBJECTED TO IN-PLANE MOMENTS

By Kazuo TAKAHASHI, Yoshihiro NATSUAKI**, Yasunori KONISHI*** and Michiaki HIRAKAWA*****

Buckling of an annular sector plate subjected to equal and opposite moments at the radial edges is examined. The governing differential equation of the plate is solved by a Galerkin method. Buckling moments and buckling modes are obtained for the annular sector plate with simply-supported radial edges and arbitrary boundary conditions along the circumferential edges.

Numerical results are shown for various geometrical parameters and three different boundary conditions. Moreover, the buckling properties of an annular sector plate are compared with those of a rectangular plate and a circular beam.

Keywords: *buckling, annular sector plate, Galerkin method*

1. INTRODUCTION

It is well known that plate structures subjected to in-plane time varying loads will execute violent out-of-plane vibrations, although the amplitude of the excitation is much less than the corresponding static critical load[1]. This phenomenon is called parametric excitation or dynamic instability. It is necessary to examine the vibration and buckling properties of the target structures previous to dynamic stability analysis.

Although many researchers have studied bending and vibration of an annular sector plate, investigations on the buckling problem have been rather scanty. Rubin[2] has considered an annular sector plate subjected to constant in-plane forces along the radial and angular directions. Srinvasan et al.[3] have presented the buckling of an annular sector plate subjected to uniform forces along the circumferential edges. Harik[4] has presented the buckling of an annular sector plate with clamped radial edges compressed with a uniformly distributed load. Chu[5] and Mikami et al.[6] have studied the local buckling of the web plate of a circular curved beam with an I-section subjected to in-plane moments, axial and shearing forces. However, the buckling properties of an annular sector plate subjected to in-plane moments are not clear for various boundary conditions.

In this paper, the buckling of an annular sector plate with simply supported radial edges and arbitrary boundary conditions along the circumferential edges subjected to in-plane moments along the radial edges is

* Member of JSCE, Dr. Eng., Associate Professor, Department of Civil Engineering, Nagasaki University (Bunkyo-machi 1-14, Nagasaki City)
** Member of JSCE, Manager of Research and Development Sect., Katayama Iron Works, Co., Ltd. (2-21, Minamiokajima 6-chome, Taisho-ku, Osaka)
*** Member of JSCE, Dr. Eng., Professor, Department of Civil Engineering, Nagasaki University
**** Member of JSCE, Graduate Student of Nagasaki University

analyzed. The governing differential equation, whose solution is expressed as an expansion in terms of free vibration modes, is solved by applying a Galerkin procedure.

After the convergence study of the present analysis, the influence of the in-plane forces on the buckling eigen-value is examined. Numerical results are shown for various geometrical parameters and three different boundary conditions along the circumferential edges. The buckling properties of an annular sector plate are also compared with those of a rectangular plate and a circular beam subjected to in-plane moments.

2. GOVERNING EQUATION AND BOUNDARY CONDITIONS

Fig. 1 shows an annular sector plate with the opening (subtended) angle α, outer radius a and inner radius b. The polar co-ordinates (r, θ) are taken in the neutral surface of the plate.

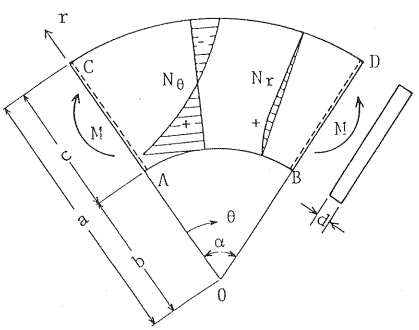

Fig. 1 Geometry and co-ordinates.

When the equal and opposite moments act along the radial edges, in-plane forces N_r, N_θ and $N_{r\theta}$ due to in-plane moments are given by using a two-dimensional problem of elasticity[7]:

$$N_r=-\frac{4M}{N}\left(\frac{a^2b^2}{r^2}\ln\frac{a}{b}+a^2\ln\frac{r}{a}+b^2\ln\frac{b}{r}\right) \quad (1)$$

$$N_\theta=-\frac{4M}{N}\left(-\frac{a^2b^2}{r^2}\ln\frac{a}{b}+a^2\ln\frac{r}{a}+b^2\ln\frac{b}{r}+a^2-b^2\right) \quad (2)$$

$$N_{r\theta}=0 \quad (3)$$

where $N=(a^2-b^2)^2-4a^2b^2(\ln(a/b))^2$ is constant and N_r, N_θ and $N_{r\theta}$ are functions of independent variable r.

The governing differential equation in the present problem can be written as[8]

$$D\nabla^4 w-\frac{1}{r}\frac{\partial}{\partial r}\left(rN_r\frac{\partial w}{\partial r}\right)-\frac{1}{r^2}N_\theta\frac{\partial^2 w}{\partial\theta^2}=0 \quad (4)$$

where $D=Ed^3/\{12(1-\nu^2)\}$ is the bending stiffness, E is Young's modulus, ν is Poisson's ratio, w is the plate deflection and $\nabla^2=\left(\frac{\partial^2}{\partial r^2}+\frac{1}{r}\frac{\partial}{\partial r}+\frac{1}{r^2}\frac{\partial^2}{\partial\theta^2}\right)$ is a Laplacian operator in the polar co-ordinates.

For simply-supported radial edges, the boundary conditions along $\theta=0$ and α are as follows:

$$w=M_\theta=0 \quad (5)$$

where M_θ is the bending moment in the angular direction.

The following three boundary conditions along the circumferential edges ($r=b$ and a) are considered in the present analysis

case I : simply-supported edges;

$$w=M_r=0 \quad (6)$$

case II : clamped edges;

$$w=\partial w/\partial r=0 \quad (7)$$

case Ⅲ : free edges;

$$M_r=V_r=0 \quad (8)$$

where M_r is the bending moment in the radial direction and V_r is the equivalent shearing force.

By denoting $\xi=r/a$, equation (4) can be expressed in the non-dimensional form

$$L(w)=\nabla^4 w+\frac{4M}{\overline{N}D}\left[\frac{1}{\xi}\frac{\partial}{\partial\xi}\left\{\xi f_1(\xi)\frac{\partial w}{\partial\xi}\right\}+\frac{1}{\xi^2}f_2(\xi)\frac{\partial^2 w}{\partial\theta^2}\right]=0 \quad (9)$$

where $\overline{N}=(1-\beta^2)^2-4\beta^2(\ln(1/\beta))^2$, $f_1(\xi)=(\beta/\xi)^2\ln(1/\beta)+\ln\xi+\beta^2\ln(\beta/\xi)$, $f_2(\xi)=-(\beta/\xi)^2\ln(1/\beta)+\ln\xi+\beta^2\ln(\beta/\xi)+1-\beta^2$ and $\beta=b/a$ is the ratio of inner to outer radii (the radius ratio).

3. METHOD OF SOLUTION

Taking these boundary conditions into account, we can express the solution of equation (9) as an expansion in terms of the free vibration modes. That is,

$$w=\sum_s a_{sn}W_{sn}(\xi,\ \theta) \quad (10)$$

in which a_{sn} is an unknown constant and W_{sn} is the eigen-function of the following equation

$$\nabla^4 W_{sn}=k_{sn}^4 W_{sn} \quad (11)$$

where k_{sn} is the eigen-value of free vibrations. Here, n is the half-wave number in the angular direction. The eigen-function is defined as[9]

$$W_{sn}=R_{sn}(\xi)\sin\alpha_n\theta \quad (12)$$

where $R_{sn}=A_{sn}J\alpha_n(k_{sn}\xi)+B_{sn}Y\alpha_n(k_{sn}\xi)+C_{sn}I\alpha_n(k_{sn}\xi)+D_{sn}K\alpha_n(k_{sn}\xi)$, in which A_{sn}, B_{sn}, C_{sn} and D_{sn} are constants of integration dependent on the boundary conditions, $J\alpha_n$ and $Y\alpha_n$ are Bessel functions, $I\alpha_n$ and $K\alpha_n$ are modified Bessel functions and $\alpha_n=n\pi/\alpha$.

Substituting equations (10) and (11) into equation (9) and applying a Galerkin procedure, one has

$$\int_\beta^1\int_0^\alpha L(w)W_{pn}\xi d\xi d\theta=0 \quad (13)$$

where $p=1, 2, \cdots N$.

Performing integrations of equation (13) and considering the orthogonality property of the eigen-function W_{sn} as shown in Appendix A, we obtain a set of equations for the unknown constant a_{pn} as follows.

$$k_{pn}^4 I_{pn}a_{pn}-(M/D)\sum_s a_{sn}I_{spn}=0 \quad (14)$$

where $I_{pn}=\int_\beta^1 R_{pn}^2\xi d\xi$, $I_{spn}=\frac{4}{\overline{N}}\int_\beta^1\left\{\xi f_1(\xi)\frac{dR_{sn}}{d\xi}\frac{dR_{pn}}{d\xi}+\frac{\alpha_n^2}{\xi}f_2(\xi)R_{sn}R_{pn}\right\}d\xi$.

Equation (14) may be written in the following matrix form

$$[I]\{X\}=(M/D)[G]\{X\} \quad (15)$$

where $\{X\}=\{a_{1n}a_{2n}\cdots a_{Nn}\}^T$ is the column vector, $[I]$ is the unit matrix and $[G]$ is the square matrix.

By introducing the notation $\lambda_{cr}=M/D$, equation (15) can be transformed into an eigen-value problem with respect to the matrix $[G]$:

$$[G]\{X\}=\lambda\{X\} \quad (16)$$

where $\lambda=1/\lambda_{cr}$.

The geometrical parameters in the present analysis are the opening angle α and the radius ratio β. In order to compare the buckling properties of an annular sector plate with those of a rectangular plate, it will be better to define the aspect ratio of an annular sector plate which denotes the ratio of the mean arc length $l=(a+b)\alpha/2$ to the loaded edge length c as

$$\mu=\frac{l}{c}=\frac{\alpha(1+\beta)}{2(1-\beta)} \quad (17)$$

4. NUMERICAL RESULTS

(1) Convergence study

Fig. 2 shows the convergency of the present solution for the annular sector plate with the radius ratio $\beta=0.5$. In this figure, the notations case-a and case-b correspond to the buckling eigen-values of the annular sector plate subjected to positive and negative moments, respectively. The solution of case-a is obtained for the opening angle $\alpha=\pi/10$ in which the solution is close to the minimum buckling eigen-values of cases I and II, while the solution of case-b is obtained for $\alpha=\pi/2$. The five-term solutions for cases I and II and the two-term solutions for case III converge for both case-a and case-b as shown in Fig. 2.

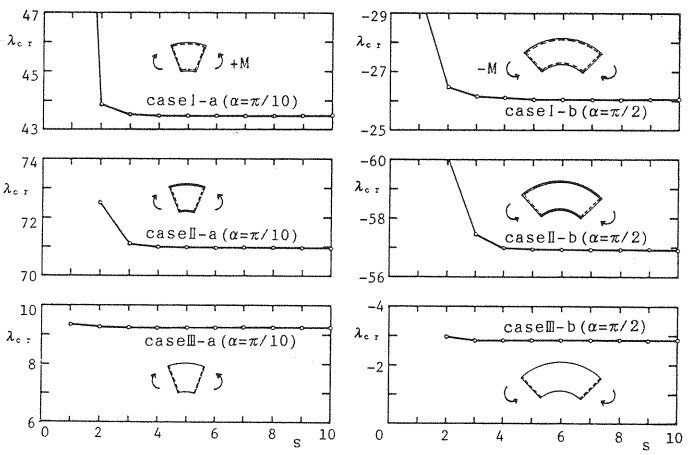

Fig. 2 Convergency of buckling eigen-values : $\beta=0.5$.

Table 1 Comparison of present solution with previous solutions : $\beta=0.5$.

case	present solution	Mikami et al.[6]	Chu[5]
I-b ($\alpha=\pi/2$)	−26.1	−26	−26.2
II-b ($\alpha=\pi/2$)	−56.9	−57	
I-a ($\alpha=\pi/10$)	43.5	43	
II-a ($\alpha=\pi/10$)	71.0	70	

Table 1 shows the comparison of the present solution with the previous solutions obtained by Chu[5] (based on the Ritz method) and Mikami et al.[6] (based on the power series method). In this table, the solutions of Mikami et al. are taken from the figures in reference[6] (Fig. 9 through Fig. 12). The present solutions agree well with the previous solutions as shown in Table 1.

Consequently, it is shown that the present solution converges rapidly and its accuracy is good. The present method is useful to clarify the buckling problem of the annular sector plates with arbitrary boundary conditions.

(2) The influence of in-plane forces (N_r, N_θ) on buckling eigen-values

Fig. 3 shows the variation of the maximum in-plane forces $N_{\theta a}$, $N_{\theta b}$ and N_{r1} with the radius ratio β for the annular sector plate subjected to the in-plane positive moment. The in-plane force N_r in the radial direction is compressive when the applied moment is negative (case-b). The maximum in-plane forces $N_{\theta b}$ and N_{r1} rapidly increase with a decrease of the radius ratio β.

In order to examine the influence of in-plane forces on the buckling eigen-values, the annular sector plate neglecting either in-plane force N_r or N_θ is analyzed for $\beta=0.5$ as shown in Fig. 4. In this figure, the buckling curves neglecting the in-plane force N_r or N_θ are shown by thin lines. Thicker lines correspond to the exact buckling curves which consider both in-plane forces. Moreover, chain lines and solid lines

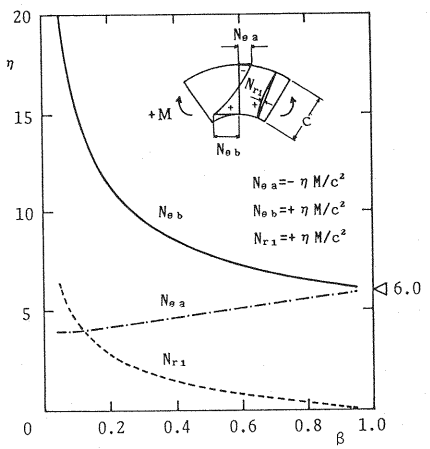

Fig. 3 Variation of maximum in-plane forces with radius ratio.

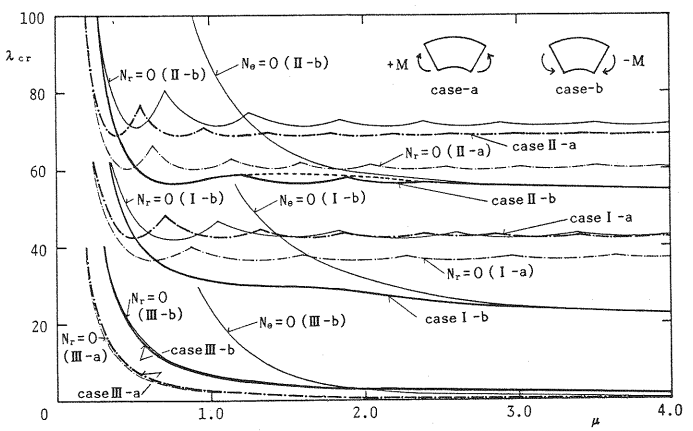

Fig. 4 Influence of in-plane forces on the buckling eigen-value : $\beta=0.5$.

indicate case-a and case-b, respectively. Of course the eigen-value of case-b is negative.

For cases I and II, the in-plane force N_r influences the buckling eigen-values as pointed out in reference[6]. In the case of buckling curves neglecting N_r, the buckling curves due to the positive moment (case-a) lie below those due to the negative moment (case-b) in contrast with the exact buckling curves. The buckling curves considering only the effect of N_r are monotonic curves and coincide with the exact buckling curves in relatively large aspect ratio μ as shown in Fig. 4, although N_{r1} is less than 25 % of $N_{\theta a}$ (see Fig. 3).

On the other hand, N_θ influences the buckling eigen-values of case III. The exact buckling curves coincide with the buckling curves considering only the effect of N_θ because there are no restraints along the circumferential edges where N_θ has a maximum value.

(3) Buckling properties of the annular sector plate

Fig. 5 through Fig. 8 show the variation of the buckling eigen-value λ_{cr} with the aspect ratio μ for the annular sector plates with radius ratios $\beta=0.8$, 0.6, 0.4 and 0.2. In these figures, the notation n denotes the half-wave number in the angular direction.

The buckling curves for $\beta=0.8$ shown in Fig. 5 are similar to those of the rectangular plate[10]. That is, the buckling curves of case I or case II have the same minimum eigen-value which is independent of the half-wave number n, and the buckling eigen-values of case III decrease monotonically with increase of μ.

Since the in-plane force N_r grows with a decrease of β, the difference in buckling curves between case-a

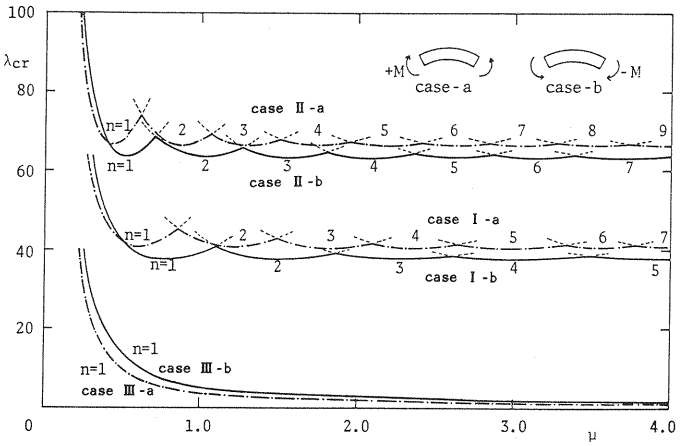

Fig. 5 Variation of buckling eigen-value with aspect ratio : $\beta=0.8$.

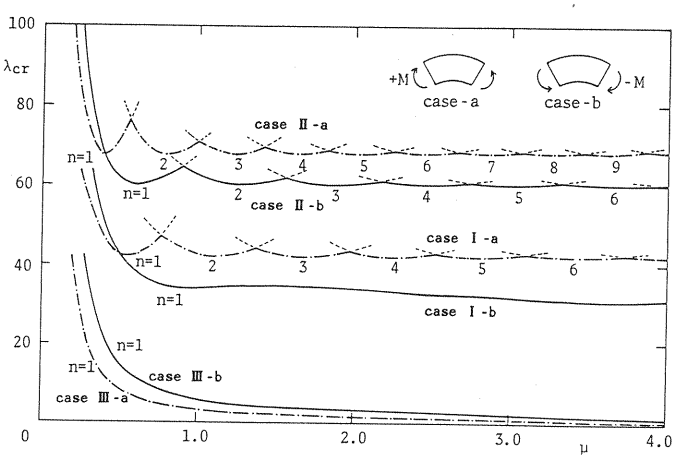

Fig. 6 Variation of buckling eigen-value with aspect ratio : $\beta=0.6$.

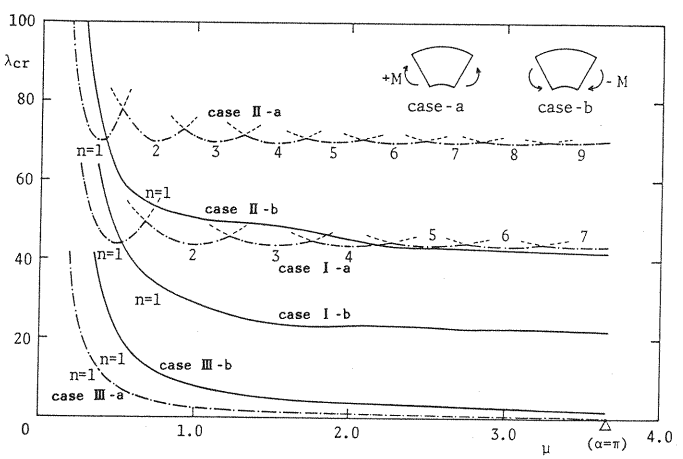

Fig. 7 Variation of buckling eigen-value with aspect ratio : $\beta=0.4$.

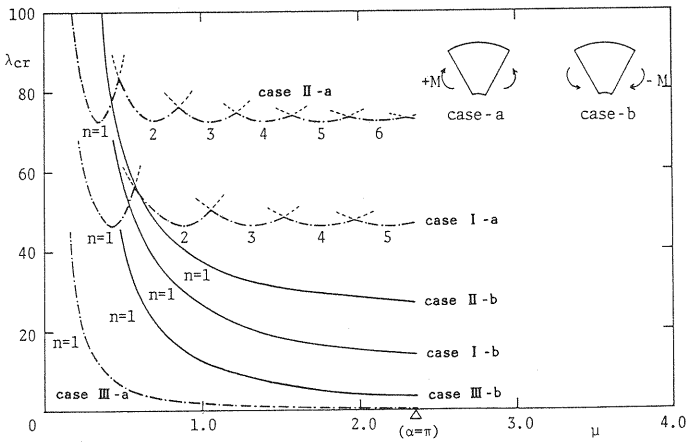

Fig. 8 Variation of buckling eigen-value with aspect ratio : $\beta=0.2$.

and case-b become larger for each case. Moreover, the buckling curves of case Ⅰ-b and case Ⅱ-b transfigure into the monotonic curves. Thus, the buckling properties of the annular sector plate are dependent on the radius ratio β.

Fig. 9 shows the buckling modes of an annular sector plate with $\alpha=\pi/3$ and $\beta=0.2$ subjected to positive and negative moments. The deflection of the compressive force region is larger than that of the tensile force region. The buckling modes are the local elastic deformation shapes except for case Ⅲ-a, in which the mode consists of rigid body deformation. Therefore, the buckling eigen-values of case Ⅲ-a are less than those of case Ⅲ-b.

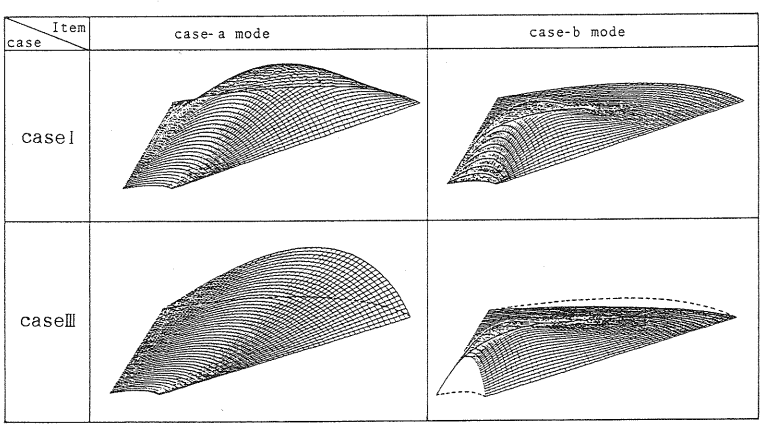

Fig. Buckling modes due to positive and negative moments : case Ⅰ and case Ⅲ with $\beta=0.2$ and $\alpha=\pi/3$.

(4) Comparison of cases Ⅰ and Ⅱ with a rectangular plate

Fig. 10 summarizes the relation between the minimum buckling eigen-value λ_{cr} and the radius ratio β for an annular sector plate whose buckling curves are the same pattern as that of a rectangular plate. The buckling coefficients of a rectangular plate having the same boundary and loading conditions are also shown in Fig. 10. The minimum buckling eigen-values of cases Ⅰ and Ⅱ are different from that of the rectangular plates with a decrease of radius ratio β. It is impossible to estimate the buckling moments of an annular sector plate by using the rectangular plate analogy when the radius ratio β is less than 0.8.

(5) Comparison of case Ⅲ with a circular beam

An annular sector plate with a very large radius ratio may be regarded as a circular beam. The

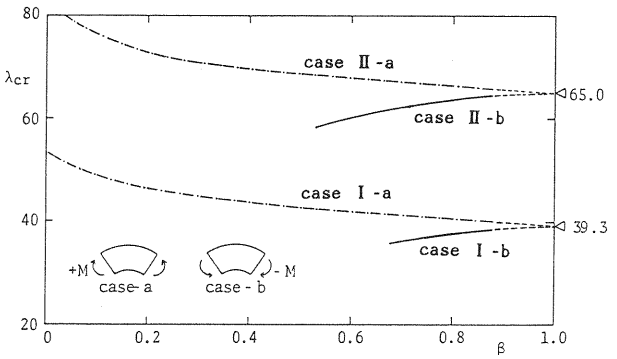

Fig. 10 Variation of minimum buckling eigen-value with radius ratio.

bending-torsional buckling moment of a circular beam[10], which consists of the rectangular cross-section (thickness d, height c) and Poisson's ratio $\nu=0.3$, is given by

$$\lambda_{cr}=\frac{M_{cr}}{EI}=\frac{1.269}{\mu'}\pm\sqrt{\left(\frac{0.269}{\mu'}\right)^2+1.538\left(\frac{\pi}{\mu}\right)^2} \quad \cdots\cdots (18)$$

where $\mu'=(1+\beta)/\{2(1-\beta)\}$.

Fig. 11 shows a comparison of the buckling eigen-values between the present solution for case Ⅲ with $\beta=0.6$ and the bending-torsional buckling eigen-value of a circular beam calculated by equation (18). The buckling eigen-value of the annular sector plate subjected to a positive moment (case-a) can be estimated by the beam theory as shown in Fig. 11 even when the plate has such high cross-section as $\beta=0.6$. On the other hand, the solution of the beam theory is different from that of the thin plate theory for case-b with $\mu<2.0$. This may be because the buckling mode of an annular sector plate subjected to a positive moment (case-a) consists of a rigid body deformation the same as a circular beam based on the beam theory (see Fig. 9).

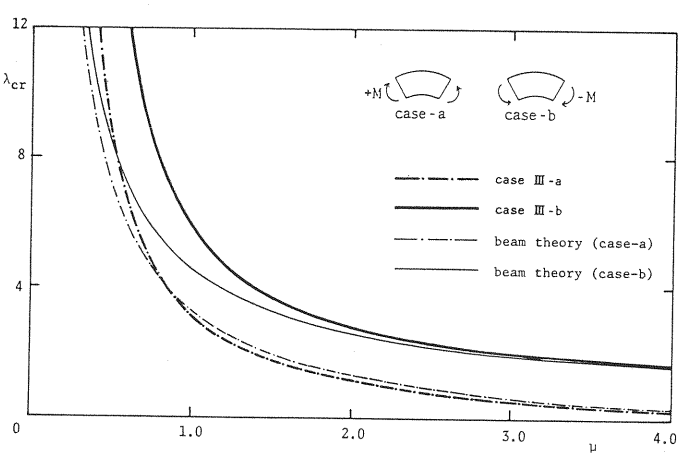

Fig. 11 Comparison of buckling eigen-value for case Ⅲ with beam theory solution : $\beta=0.6$.

5. CONCLUSIONS

In the present paper, the buckling problem of an annular sector plate subjected to in-plane moments along the radial edges is analyzed. The conclusions are as follows.

(1) In the case of an annular sector plate simply-supported or clamped along the circumferential

edges, the buckling eigen-value due to the negative moment is smaller than that due to the positive moment under the influence of an in-plane force in the radial direction.

(2) It is impossible to estimate the buckling moment of an annular sector plate with simply-supported or clamped edges by using a rectangular plate analogy when the radius ratio is less than 0.8.

(3) The buckling eigen-value of an annular sector plate, free along the circumferential edges, is influenced by an in-plane force in the angular direction.

(4) The buckling eigen-value of an annular sector plate with the free edges subjected to a positive moment agree well with the bending-torsional buckling moment of a circular curved beam when the radius ratio is greater than 0.6.

APPENDIX A : Integrations involved in a Galerkin procedure

(1) Orthogonality property of the eigen-function of the annular sector plate

$$\int_\beta^1 R_{sn}R_{pn}\xi d\xi \begin{cases} =0 & (s\neq p) \\ =I_{sn} & (s=p) \end{cases} \quad \cdots\cdots (A\cdot1)$$

(2) Definite integral

$$\int_\beta^1 \frac{1}{\xi}\frac{d}{d\xi}\left\{\xi f_1(\xi)\frac{dR_{sn}}{d\xi}\right\}R_{pn}\xi d\xi = \left|\xi f_1(\xi)\frac{dR_{sn}}{d\xi}R_{pn}\right|_\beta^1 - \int_\beta^1 \xi f_1(\xi)\frac{dR_{sn}}{d\xi}\frac{dR_{pn}}{d\xi}d\xi$$

$$= -\int_\beta^1 \xi f_1(\xi)\frac{dR_{sn}}{d\xi}\frac{dR_{pn}}{d\xi}d\xi \quad \cdots\cdots (A\cdot2)$$

REFERENCES

1) Bolotin, V. V. : The Dynamic Stability of Elastic Systems, San Francisco, Holden-Day Inc., 1964.
2) Rubin, C. : Stability of Polar-Orthotropic Sector Plates, Journal of Applied Mechanics, Vol. 45, No. 2, pp. 448~450, 1978.
3) Srinivasan, R. S. and Thiruvenkatachari, V. : Stability of Annular Sector Plates with Variable Thickness, American Institute of Aeronautics and Astronautics Journal, Vol. 22, No. 2, pp. 315~317, 1984.
4) Harik, I. E. : Stability of Annular Sector Plates with Clamped Radial Edges, Journal of Applied Mechanics, Vol. 52, No. 4, pp. 971~972, 1985.
5) Chu, K. Y. : Beuluntersuchung von ebenen Stegblechen Kreisförmig gekrümmter Träger mit I-Querschnitt, Stahlbau, Heft 5, S. 129~142, 1966.
6) Mikami, I., Akamatsu, Y. and Takeda, H. : Elastic Local and Coupled Buckling of Vertically Curved I-Girders under Pure Bending, Proc. of JSCE, Vol. 230, pp. 45~54, 1974.
7) Timoshenko, S. P. and Gere, J. M. : Theory of Elastic Stability, 2nd ed., McGraw-Hill Book Co., Inc., New York, N. Y., 1961.
8) Natsuaki, Y., Takahashi, K., Konishi, Y. and Hirakawa, M. : Buckling of an Annular Sector Plate Subjected to Inplane Moment, Journal of Structural Engineering, Vol. 34 A, pp. 181~190, 1988.
9) Yamasaki, T., Chisyaki, T. and Kaneko, T. : Free Transverse Vibration of Circular Ring Sector Plates, Technology Reports of the Kyushu University, Vol. 42, No. 4, pp. 576~583, 1969.
10) Column Research Committee of Japan : Handbook of Structural Stability, Corona Publisher Co., Ltd., 1971.

(Received July 4 1988)